

## STATUS OF MSBS STUDY AT NAL IN 1995

Hideo SAWADA, Hisasi SUENAGA, Tetuya KUNIMASU, Takashi KOHNO  
National Aerospace Laboratory (Japan)  
7-44-1 Jindaijihigashi-machi Chofu-shi Tokyo 182, Japan

### SUMMARY

Magnetic field intensity and currents passing through the coils of the National Aerospace Laboratory (NAL) 10cm Magnetic Suspension and Balance System (MSBS) were measured while a cylindrical model was oscillated along x,y,z and also about y and z axes, respectively. The model was made of alnico 5 and was 8mm in diameter and 60mm long. Two kinds of tests were carried out. Amplitude of the oscillation was varied at a frequency of 10Hz. Frequency was varied from 1 to 50Hz in the other test. Results of the tests show that the relation between coil currents and magnetic force acting on the model is affected by frequency. They also show that the relation between measured magnetic field intensity and the force in vertical direction is independent of the frequency below 30Hz. Using the measured magnetic field intensity, the vertical force can be evaluated at the MSBS instantaneously when a model moves at frequencies below 30Hz. A static drag force calibration test was carried out at the 60cm MSBS. Obtained relationships between measured drag coil currents and loads shows large hysteresis.

### INTRODUCTION

Magnetic Suspension and Balance Systems (MSBS) are a kind of model support system of wind tunnels for supporting a model in flow with magnetic force. It can avoid the model support interference because the flow field in a test section will not be affected by the magnetic field except for some very high speed flow, etc. Magnetic field for suspending a model is generated by currents passing through some coils arranged around a test section. Then the magnetic force acting on the model corresponds to the currents. When the model is at a fixed position in the flow, the magnetic force must balance with the aerodynamic force acting on the model plus the gravity force. This means that the system can work as a balance for the aerodynamic force by measuring the coil currents. The relation between the magnetic force and coil currents can be decided uniquely by some calibration tests (static force calibration tests) in almost all cases. In case of a model in motion, the difference between the magnetic force and the aerodynamic force places the model in motion. Then the aerodynamic force can be evaluated by subtracting the force driving the model motion from the magnetic force. The inertia force can be estimated by measuring model motion. This means that the system can measure dynamic force. It is also easy for the system to get accurate model position because it uses the position data for its control. It is easy to create suitable forces on a model by placing the model in suitable motion in the system. The tests corresponding to the magnetic force to coil currents are called dynamic force calibration tests. Dynamic calibration tests can replace static force tests because there is no difference between the

force driving the model motion and the force by pulling with threads in the sense of the force acting on the model. Some dynamic force calibration tests were carried out at the 10cm MSBS. Preliminary static force calibration tests were conducted at the 60cm MSBS.

## SYMBOLS

$g$	gravity acceleration ( $= 9.8\text{m/sec}^2$ )
$H$	magnetic field intensity, $(H_x, H_y, H_z)$ (T)
$H_i$	a magnetic field intensity component at a position along the coil no. $i$ axis. (T) See Figure 2.
$H_{\text{monitor}}$	$x$ component of the magnetic field intensity inside test section (T)
$H_{\text{drag}}, H_{\text{side}}, H_{\text{lift}}, H_{\text{pitch}}, H_{\text{yaw}}$	See equation (1)
$I_i$	current passing through coil no. $i$ (A)
$I_{\text{drag}}, I_{\text{side}}, I_{\text{lift}}, I_{\text{pitch}}, I_{\text{yaw}}$	See equation (1)
$I_{yy}, I_{zz}$	moment of inertia about the $y$ and $z$ axis, respectively. ( $\text{kgm}^2$ )
$K_{\text{drag}}, K_{\text{side}}, K_{\text{lift}}, K_{\text{pitch}}, K_{\text{yaw}}$	proportional constant between force and magnetic field intensity combination. See equations (2) and (3).
$m$	model mass (kg)
$m_x$	$x$ component of magnetic moment (Wbm)
$(x, y, z)$	coordinate system. See Figure 1.
$\theta$	angle about the $y$ axis.
$\phi$	angle about the $z$ axis

## DYNAMIC FORCE CALIBRATION TEST

### Experimental Design

Magnetic field around the test section together with coil currents was measured with Hall sensors during dynamic force calibration tests. Some preliminary test results have been published. As mentioned in References 1 and 2, even the most suitable combination of measured coil currents showed differences from model position in the sense of phase. The difference was observed to depend on the motion frequency. On the contrary, a suitable combination of measured magnetic field intensity components appeared completely in phase with the model position. In this dynamic calibration test, forced oscillations of a model were performed in two ways. Frequency varied from 1 to 50Hz along the  $x, y$  and  $z$  axes and about the  $y$  and  $z$  axes in one way. The amplitude of 10Hz oscillation varies in the other way. In order to avoid the effect of eddy currents on metal test section walls, the test section was removed during the test.

The model is 60mm long and 8mm in diameter and of alnico 5 permanent magnet. In order to measure the model position, the model was wrapped with thin white paper. The paper measured 0.2g +/- 0.1g in mass. The shape is 60mm high x 52mm wide x 0.1mm thick. A 4mm wide black line was printed along the center line of the paper. The line is used to measure the  $x$  position of the model. The whole mass of the model including the paper was measured as 23.8g +/- 0.1g with

a balance. The inertia moment of the model was evaluated at  $2.87 \times 10^5 \text{kgm}^2$  about an axis through the gravity center normal to the model axis by calculation from the model shape and mass. The model was supported by the control of 5 degrees of freedom except for rolling motion about the model axis. Besides, constant currents of 4 A in magnitude pass through the 4 side coils to generate an additional constant magnetic field which makes model position stable in  $y$  and  $\phi$ .

The model was suspended at the center of the 10cm MSBS which is the coordinate system origin. All oscillations were pure sinusoidal, pure heaving and pure pitching motions. In the pitching (and yawing) motions, the center of gravity was controlled to be kept at the origin.

Coil currents were measured from monitor outputs of 10 power amplifier units. In order to evaluate the monitor output accuracy, they were compared between 0 to 50Hz with the currents measured with a zero inductance Shunt type resistance of  $0.1 \Omega$  and of 0.1% accuracy. The monitor outputs are less than the coil currents by about 1.2% but the difference is independent of the frequency. The monitor outputs were delayed against the real coil currents by 0.5 degree at the highest frequency of 50Hz.

The monitor outputs were measured and recorded in a personal computer with 12 bit AD converters with sample and hold function which are 0.2% accurate over a +/- 10V range. All converters were adjusted to 5mV error at most in their whole range with a reference voltage generator of 0.01% accuracy. The coil currents and the magnetic field intensity components were measured at the same time.

The Hall sensors, THC126 (Toshiba), were used to measure the magnetic field intensity components at the 8 points shown in Figure 2.  $H_x$  is symbolized as  $H_y$  here. Although the measurement of  $H_y$  is not disturbance-free against the flow field, it is possible to measure  $H_y$  like a wake survey in wind tunnel tests without serious affect on the test result. The sensors were driven in the constant current mode. They were calibrated with the model 9903 of F.W. BELL which is 0.1%FSR accurate. They showed good linearity between the Hall sensor outputs and the Gauss meter output. An example of the calibration test results are shown in Figure 3.

The model position was measured with an in-house-developed model position sensing system. The system was described in detail in Reference 3. The position sensor was calibrated by a calibration model of 8mm diameter wrapped with the same paper as the dynamic force calibration model. It was positioned on a stage which can vary all positions in 6 degree of freedom. Some examples of the position sensor calibration test are shown in Figure 4. There are some interferences between measured positions, particularly in  $y$  and  $\phi$ . The interference will induce some unexpected motion of the model.

The control speed of the MSBS measured 489.8Hz. The obtained model position by the sensor is delayed by 3.0ms from the measuring time of the coil currents because it is estimated

with CCD sensors as presented in Figure 5. The times and frequencies shown in the figure were measured with a universal pulse counter.

### Dynamic Force Calibration Analysis

The model is assumed a perfect cylinder and is also assumed to be magnetized along the model axis like  $(m_x, 0, 0)$ . The magnetic force components along the  $x, y$  and  $z$  directions acting on the suspended model can be approximated by the magnetic field intensity gradient about the model multiplied with  $m_x$ . The moments about the  $y$  and  $z$  axes can be also approximated by the magnetic field intensity about the model multiplied with  $(m_x, 0, 0)$ . Then the moment components about the  $y$  and  $z$  axes are approximately proportional to the averaged  $H_z$  and  $H_y$  over the model, respectively. To monitor the magnetic field intensity about the model, the following combinations of the measured magnetic field intensity components are defined:

$$\begin{aligned}
 H_{drag} &= \frac{H_1 + H_2 - H_3 - H_4 + H_5 + H_6 - H_7 - H_8}{8}, \\
 H_{monitor} &= H_9, & I_{drag} &= \frac{I_0 + I_9}{2}, \\
 H_{side} &= \frac{H_2 + H_4 - H_6 - H_8}{4}, & I_{side} &= \frac{I_2 + I_4 + I_6 + I_8}{4}, & \dots & (1) \\
 H_{lift} &= \frac{H_1 + H_3 - H_5 - H_7}{4}, & I_{lift} &= \frac{I_1 + I_3 + I_5 + I_7}{4}, \\
 H_{pitch} &= \frac{H_1 + H_3 + H_5 + H_7}{4}, & I_{pitch} &= \frac{I_1 + I_3 - I_5 - I_7}{4}, \\
 H_{yaw} &= \frac{H_2 + H_4 + H_6 + H_8}{4}, & I_{yaw} &= \frac{I_2 + I_4 - I_6 - I_8}{4}.
 \end{aligned}$$

The motion of the model gravity center satisfies the following equations:

$$\begin{aligned}
 m\ddot{x} &= K_{drag} \cdot H_{drag}, \quad \text{or} \quad m\ddot{x} = K_{monitor} \cdot H_{monitor}, \\
 m\ddot{y} &= K_{side} \cdot H_{side}, & \dots & (2) \\
 m\ddot{z} &= K_{lift} \cdot H_{lift} - mg,
 \end{aligned}$$

where  $K$ 's are proportional constants between the quantities defined above and the corresponding force. The motion of model rotation about the  $y$  and  $z$  axes at the gravity center satisfies the following equations:

$$\begin{aligned}
 I_{yy} \ddot{\theta} &= K_{pitch} \cdot H_{pitch}, \\
 I_{zz} \ddot{\psi} &= K_{yaw} \cdot H_{yaw}, & \dots & (3)
 \end{aligned}$$

where  $K$ 's are the similar ones as above mentioned. If motion is sinusoidal, the force driving the model motion varies sinusoidally as the motion. Besides, the motion and the force must be in

phase. The model was forced to make as pure a sinusoidal motion as possible in the dynamic force calibration test. By examining the phase between the motion and the quantities defined in the above equations, it can be estimated whether or not the quantities are suitable for evaluating the dynamic force.

## Dynamic Force Calibration Test Results

### Heaving Motion

Figure 6 shows trajectories of  $H_{lift}$ ,  $I_{lift}$  and  $z$  position of the model with respect to time during a 10Hz heaving motion. The three quantities are normalized with their rms values.  $H_{lift}$  and  $z$  are perfectly in phase. The waveforms of the two also look like a single frequency sinusoidal oscillation. Figure 7 shows also  $H_{lift}$ ,  $I_{lift}$  and  $z$  vs. time during a 20Hz heaving motion. The same observation can be remarked as in the 10Hz motion. This fact confirms that  $H_{lift}$  is directly proportional to the force in the  $z$  direction. On the contrary, there is observed apparent phase difference between  $-I_{lift}$  and  $z$ . This suggests that  $I_{lift}$  is not proportional to the force unlike  $H_{lift}$ .

The rms value of the force during the heaving motion was evaluated from the measured  $z$  position of the model. Figure 8 shows the relation between  $H_{lift}$  and the force in their rms values. The symbol of  $x$  shows the case of changing amplitude of 10Hz heaving motion. A dotted line in the figure is a least square approximation line fitted to the results in the amplitude change case. The symbol of an open circle shows the case of changing frequency between 1 to 30Hz with various amplitudes. The open circles are on the approximation line except for frequencies less than 5Hz. The results at frequencies higher than 30Hz are not on the line. One of the causes is poor magnetic field control because of large induced electromotive force. The maximum error of the dynamic force balance in the  $z$  direction reduces to about 2.4% in the region of the figure. The error is observed in a 1Hz heaving motion and its value is 2mN. The change of coil currents is about the resolution of the current amplifier units at the frequency. Then, suitable control of the magnetic field cannot be expected. The fact suggests that a core permanent magnet must be chosen to meet test requirements. When a small force in the  $z$  direction is measured, a weaker and light magnet must be used.

Figure 9 also shows that relation between the force and  $I_{lift}$  in their rms values. The symbols are the same as in Figure 8. Although the results in the case of amplitude change are on a line, the results in the case of frequency change are not. They show a frequency dependence when the frequency is higher than 10Hz. It means that the obtained data must be compensated by the effect of frequency dependence if dynamic force is estimated with  $I_{lift}$ . The magnetic circuits of the 10cm MSBS are made of iron blocks and have hysteresis loss dependent on frequency. This is suspected to be the cause of the frequency dependence.

## Pitching Motion

Figure 10 shows trajectories of  $H_{pitch}$ ,  $I_{pitch}$  and  $\theta$  of the model attitude with respect to time during 10Hz pitching motion. The three quantities are normalized with their rms values.  $H_{pitch}$  and  $\theta$  are in phase. The waveforms of the two also look like single frequency sinusoidal oscillations. Figure 11 shows also  $H_{pitch}$ ,  $I_{pitch}$  and  $\theta$  vs. time during 20Hz pitching motion. Although  $H_{pitch}$  and  $\theta$  are in phase independently of frequency,  $H_{pitch}$  trajectory differs from a pure sinusoidal waveform around its peaks.  $H_{pitch}$  is approximately proportional to the torque about the y axis according to the figures. On the contrary, there is observed apparent phase difference between  $I_{pitch}$  and  $\theta$ . This suggests that  $I_{pitch}$  is not proportional to the torque unlike  $H_{pitch}$ .

The rms value of torque about the y axis (pitching moment) was evaluated from the measured  $\theta$ . Figure 12 shows the relation between the pitching moment and  $H_{pitch}$  in their rms values. The symbols are the same as in the case of the heaving motion test. The open circles are not on the approximation line. The similar difference between the two kinds of tests is found in the relation between pitching moment and  $I_{pitch}$  as shown in Figure 13. The difference is larger than in Figure 12 with pitching moments larger than 0.7mNm. It suggests that the frequency dependence lies in the moment evaluation by  $I_{pitch}$  as in the heaving motion test. The open circles and cross symbols in the range less than the pitching moment of 0.2mNm are not on a line. The cause is that  $I_{pitch}$  and  $H_{pitch}$  are very small and nearly out of the controllable range. Figure 14 shows the  $H_{pitch}$ ,  $I_{pitch}$  and  $\theta$  vs. time during 4Hz pitching motion. The model position is controlled but  $H_{pitch}$  and  $I_{pitch}$  are scattered around the pitch angle trajectory. The other open circles are approximately on a line but the line is different from the line approximated by the cross symbols. It means the relation between pitch angle and  $H_{pitch}$  depends on the frequency. The cause of it has not yet been isolated.

## Oscillation in the x direction

Figure 15 shows  $H_{drag}$ ,  $I_{drag}$ , and  $H_{monitor}$  and x position with respect to time during 10Hz oscillating motion in the x direction. The four quantities are normalized with their rms values. Either of four is not perfectly in phase with z.  $H_{monitor}$  is the most in phase with z of the three. The rms value of the force in the x direction was evaluated from the measured x position of the model. Figures 16, 17, and 18 show the relations between the force and  $H_{drag}$ ,  $I_{drag}$ ,  $H_{monitor}$ , in their rms values. Results in the frequency change are nearly on a line approximated by those in amplitude change at 10Hz in the case of using  $H_{monitor}$ . The other two cases show the frequency dependency. But results in the case of frequency change are nearly on a line approximated by those in amplitude change only around 10Hz in case of using  $I_{drag}$ . One of the causes is the air-cored drag coils without the hysteresis loss by iron cores.

## Oscillations in the $y$ direction and about the $z$ axis

Figure 19 shows  $H_{side}$ ,  $I_{side}$  and  $y$  position of the model with respect to time during 10Hz oscillation in the  $y$  direction. The three quantities are normalized with their rms values. Three waveforms do not look sinusoidal at all. It means that the control is not adequate. Cause of the distorted waveforms is the poor accuracy in  $y$  of the model position sensor. The rms value of force in  $y$  was evaluated from the measured  $y$  position of the model. Figures 20 and 21 show the relations between the force in the  $y$  direction and  $H_{side}$ ,  $I_{side}$  in their rms values. Results in the two test cases are scattered around a line which is approximated by the amplitude change tests at 10Hz.

Figure 22 shows  $H_{yaw}$ ,  $I_{yaw}$  and  $\phi$  position of the model with respect to time during 10Hz oscillating motion about the  $z$  axis. The three quantities are normalized with their rms values. Three waveforms do not look sinusoidal. It means that the control is not adequate. Cause of the distorted waveforms is the poor accuracy in  $\phi$  of the model position sensor. The rms value of yawing moment was evaluated from the measured  $\phi$  of the model. Figures 23 and 24 show the relations between the yawing moment and  $H_{yaw}$ ,  $I_{yaw}$  in their rms values. Results in the two test cases are scattered around a line which is approximated by amplitude change tests at 10Hz.

## STATIC FORCE CALIBRATION TEST AT THE 60CM MSBS

A preliminary static force calibration test was carried out at the 60cm MSBS. The 60cm MSBS is the largest in its test section size, which is described in References 1 and 2. It is operated in 5 degree of freedom control. But  $y$  position and yaw angle control is very slow because of poor accuracy of the model position sensor in those directions. Only axial force was calibrated by pulling the model with 100g scale weights and measuring the drag coil currents. Figure 25 shows a picture of the test. The model is 381mm long and 55mm diameter and it contains a cylindrical permanent magnet core of Fe-Cr-Co magnet which is 50mm diameter and 300mm long. In order to measure the model position, the model was wrapped with a thin white paper as in the case of the 10cm MSBS model. The whole mass of the model measured 5.1kg. The model was supported by the control of 5 degree of freedom except for rolling motion. Drag coil current was measured with monitor output of a power amplifier unit for the drag coil. The monitor outputs of the 5 power amplifiers are accurate of 0.1% FSR up to 75A for constant output. The monitor output was measured and recorded by a FFT analyzer. The model position was measured with the same typed model position sensing systems at the 10cm MSBS. The position sensor was calibrated with the model. It was positioned on a stage which can vary all positions in 6 degree of freedom. The control speed of the MSBS measured 248Hz. The obtained relation between the drag coil current and applied load is shown in Figure 26. Apparent hysteresis is observed. Drag force calibration tests were carried out several times. Hysteresis is observed every time. Figure 27 shows the results of another test in which the axial load increases and decreases in small steps of about 10g. Large hysteresis is observed.

## REMARKS

Magnetic field intensity and coil currents of the 10cm MSBS were measured when a cylindrical model was oscillated along x, y, z and also about y and z axes, respectively. Two kinds of tests were carried out. Amplitude of the oscillation varies with constant frequency of 10Hz in one mode. Frequency varies from 1 to 50Hz in the other mode.

In case of heaving motion,  $H_{lift}$  and z position are in phase but  $I_{lift}$  and z are out of phase. The relation between  $H_{lift}$  and the force in z direction is very linear in the tested range and is also independent of the frequency below 30Hz at the 10cm MSBS. On the contrary, the relation between  $I_{lift}$  and the force is not linear but also depends on the oscillation frequency.  $H_{lift}$  can be used for estimating lift force acting on a model in motion.

In case of pitching motion,  $\theta$  trajectory looks like a pure sinusoidal waveform but  $H_{pitch}$  trajectory differs from a pure sinusoidal waveform around its peaks although  $H_{pitch}$  and  $\theta$  are in phase.  $I_{pitch}$  and  $\theta$  are out of phase. The relation between  $H_{pitch}$  and pitching moment is linear but depends on the test modes. The cause of the test mode dependence has not been isolated yet. The relation between  $I_{lift}$  and the moment is not linear but also depends on the frequency.

x position trajectory looks like a good sinusoidal waveform but  $H_{drag}$ ,  $H_{monitor}$  and  $I_{drag}$  trajectories do not look like good sinusoidal waveforms. x and either of the three is not apparently in phase. The relation between  $H_{drag}$  and the force in the x direction is linear but depends on the two test modes.  $H_{monitor}$  and the force is linear and is also independent of the test mode. It suggests that the relation is independent of the frequency. The relations between  $I_{drag}$  and the force and between  $H_{drag}$  and the force are linear but depend on the test modes.

Oscillations in the y direction and about the z axis are not pure sinusoidal ones because of poor accuracy in y and  $\phi$  of the model position sensing device at the 10cm MSBS. The relations between  $H_{side}$  and the force in the y direction and between  $I_{side}$  and the force look linear but are not reliable to estimate the force from the measured  $H_{side}$  or  $I_{side}$ . The relations between  $H_{yaw}$  and the yawing moment and between  $I_{yaw}$  and the moment also look linear but are not reliable either.

At the 60cm MSBS, drag force calibration tests were carried out. The results show large hysteresis between load and drag coil current. The cause has not been isolated yet.

## REFERENCES

1. Sawada, H.; Suenaga, H.; Suzuki, T.; and Ikeda, N.: Status of MSBS Study at NAL. NASA CP-3247, May 1994, pp. 275-289.
2. Sawada, H. and Suenaga, H.: Magnetic Suspension and Balance Systems at NAL. Conference Proceedings of PICAST' 1, December 1993, pp. 1014-1021.
3. Sawada, H.; Kanda, H.; and Suenaga, H.: The 10cm x 10cm Magnetic Suspension and Balance System at the National Aeronautical Laboratory. AIAA91-0397, January 1991.
4. Eskin, J.: An Investigation into Force/Moment Calibration Techniques Applicable to a Magnetic Suspension and Balance System. NASA CR-181695, August 1988.
5. Kohno, T.; Sawada, H.; Suenaga, H.; and Kunimasu, T.: NAL 0.6m x 0.6m MSBS - the Latest Development. Proceedings of the 33rd Aircraft Symposium, November 1995, pp. 345-348.

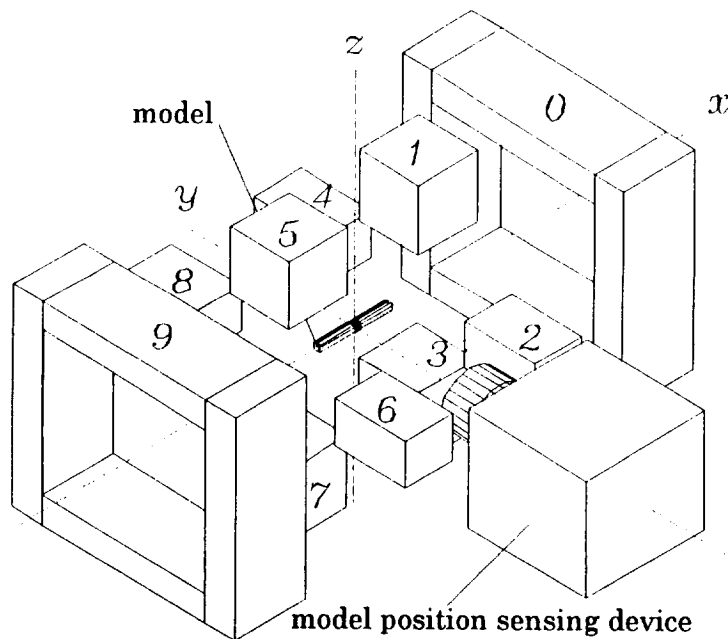


Figure 1 coil number at the 10cm MSBS

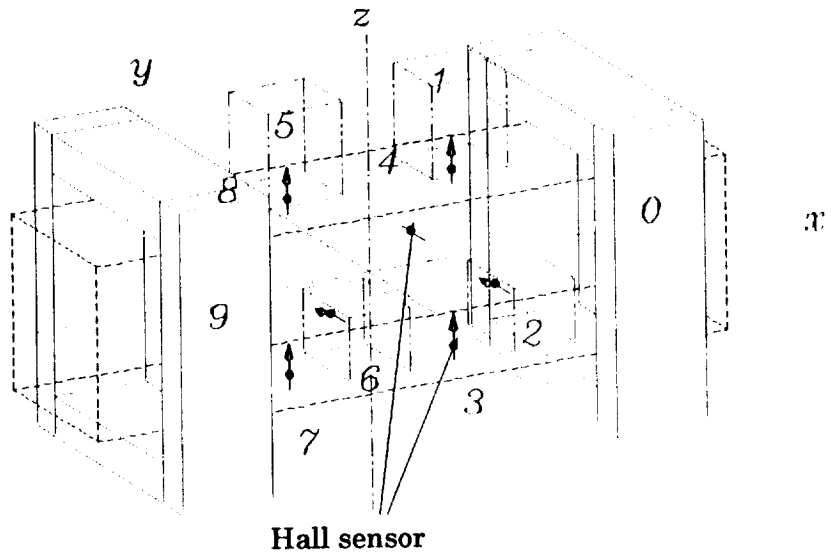


Figure 2 Hall sensor position

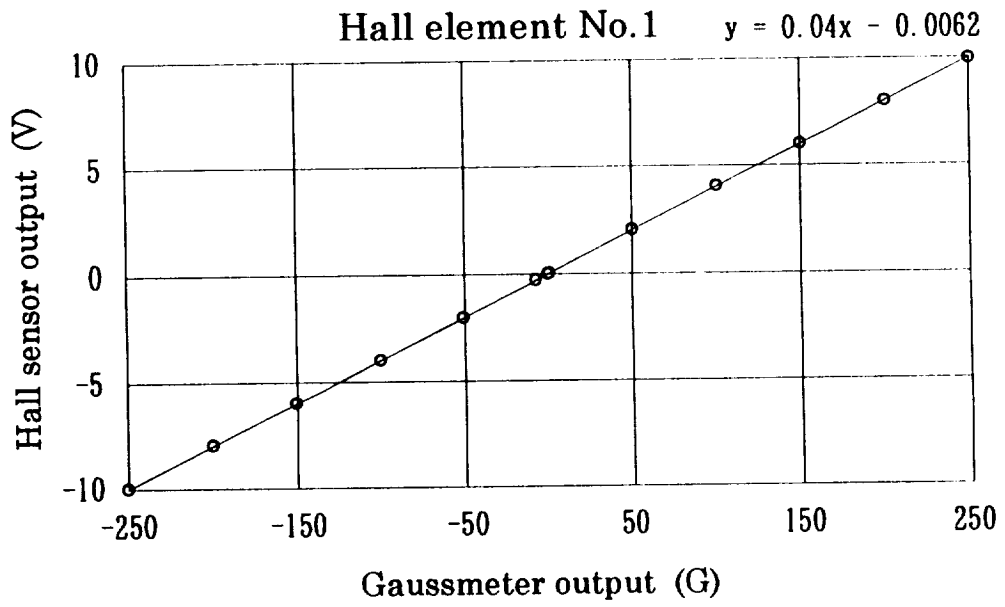


Figure 3 Hall sensor calibration test result

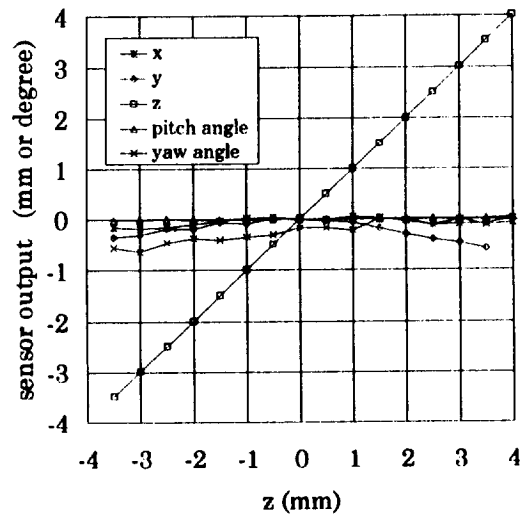


Figure 4 model position sensing device calibration test result

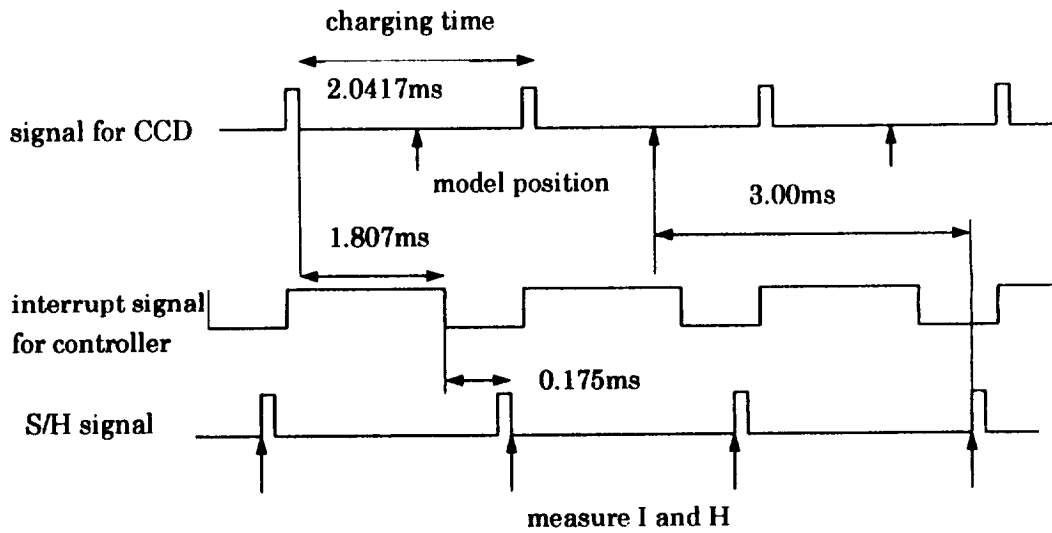


Figure 5 data acquisition timing diagram

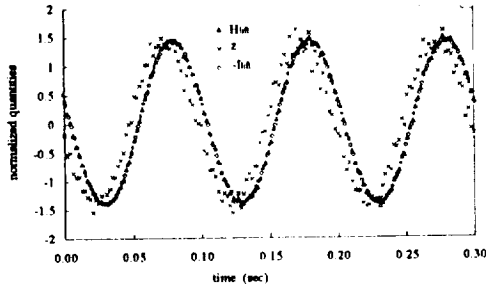


Figure 6  $z, H_{LR}, I_{LR}$  vs. time (10Hz)

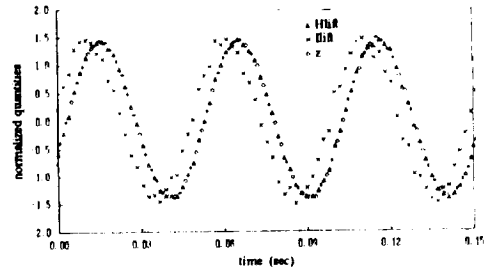


Figure 7  $z, H_{LR}, I_{LR}$  vs. time (20Hz)

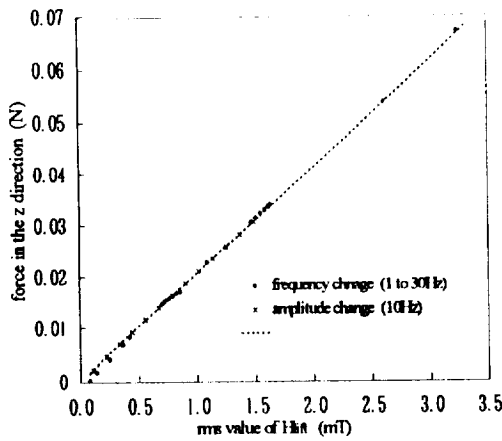


Figure 8 relation between  $H_{LR}$  and vertical force

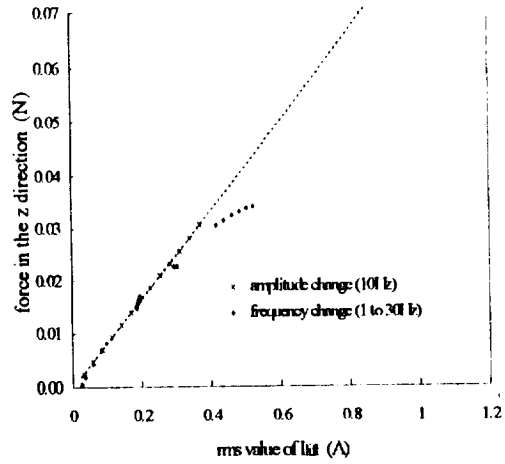


Figure 9 relation between  $I_{LR}$  and vertical force

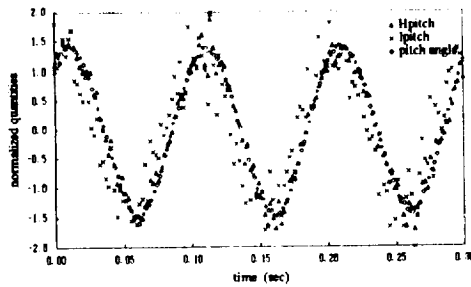


Figure 10  $\theta, H_{pitch}, I_{pitch}$  vs. time (10Hz)

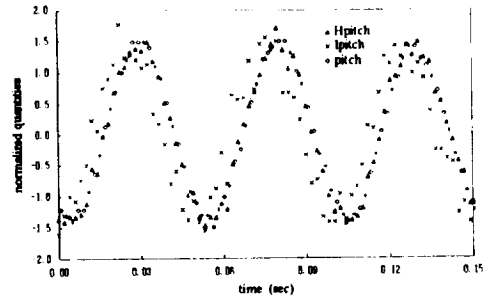


Figure 11  $\theta, H_{pitch}, I_{pitch}$  vs. time (20Hz)

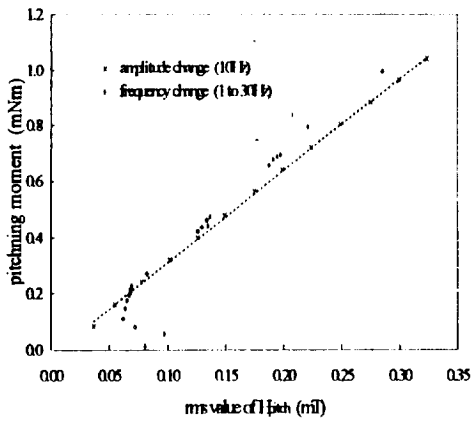


Figure 12 relation between  $H_{pitch}$  and pitching moment

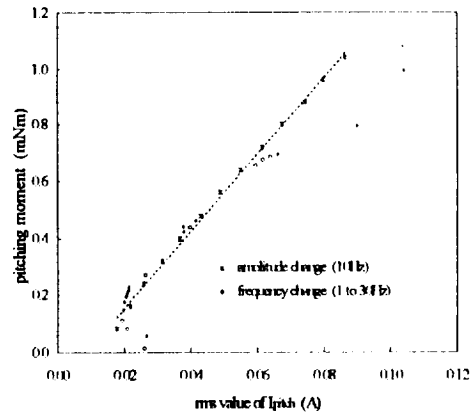


Figure 13 relation between  $I_{pitch}$  and pitching moment

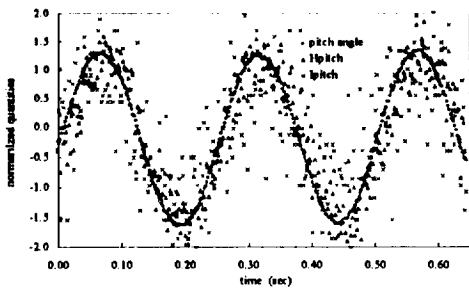


Figure 14  $\theta, H_{pitch}, I_{pitch}$  vs. time (4Hz)

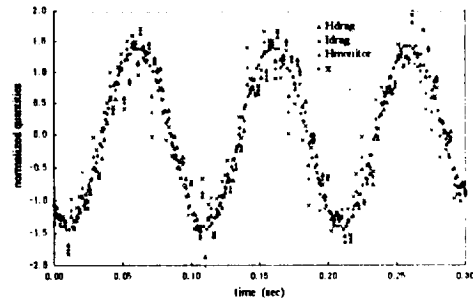


Figure 15  $x, H_{drag}, H_{monitor}, I_{drag}$  vs. time (10Hz)

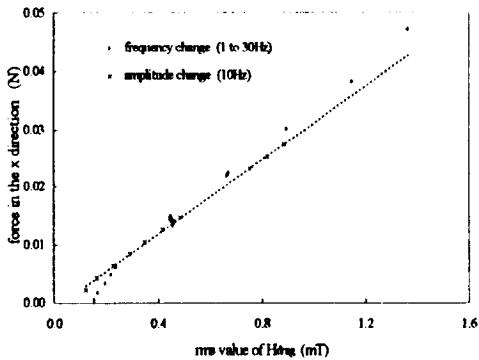


Figure 16 relation between  $H_{drag}$  and force in the x direction

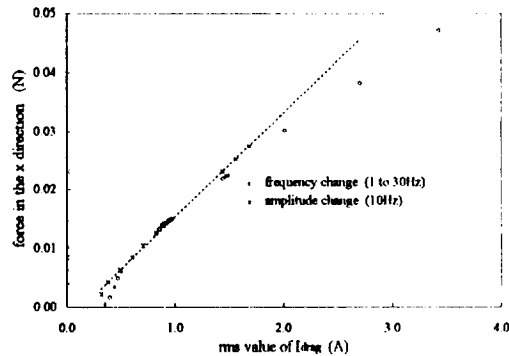


Figure 17 relation between  $I_{drag}$  and force in the x direction

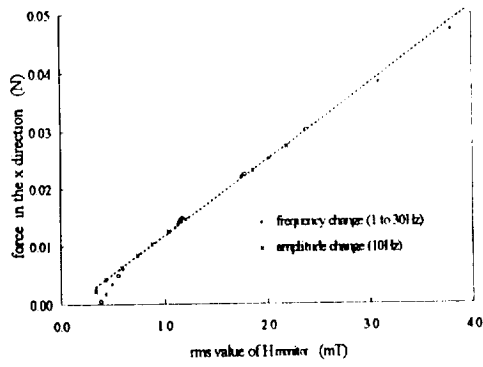


Figure 18 relation between  $H_{\text{monitor}}$  and force in the x direction

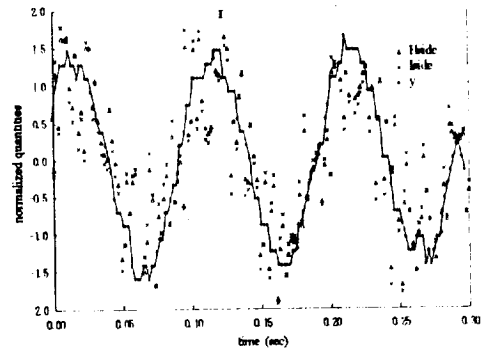


Figure 19  $y, H_{\text{side}}, I_{\text{side}}$  vs. time (10Hz)

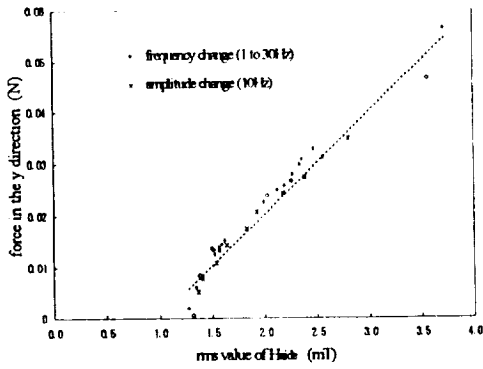


Figure 20 relation between  $H_{\text{side}}$  and force in the y direction

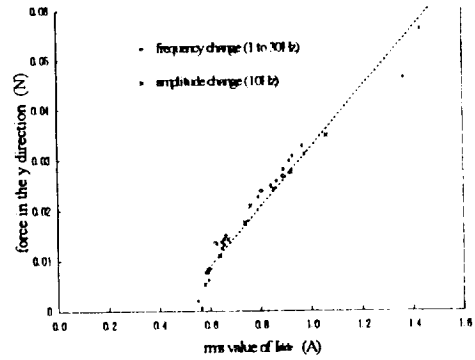


Figure 21 relation between  $I_{\text{side}}$  and force in the y direction

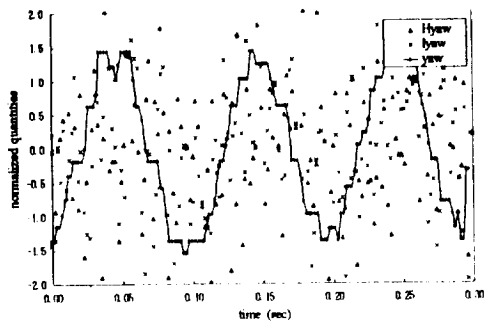


Figure 22  $\phi, H_{\text{yaw}}, I_{\text{yaw}}$  vs. time (10Hz)

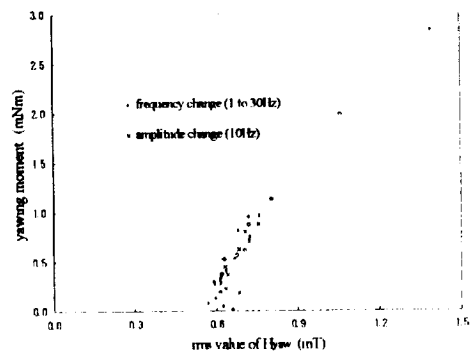


Figure 23 relation between  $H_{\text{yaw}}$  and yawing moment

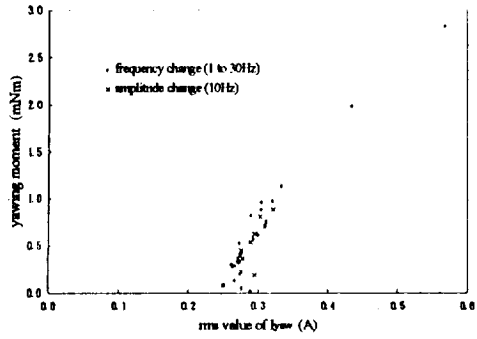


Figure 24 relation between  $I_{yaw}$  and yawing moment

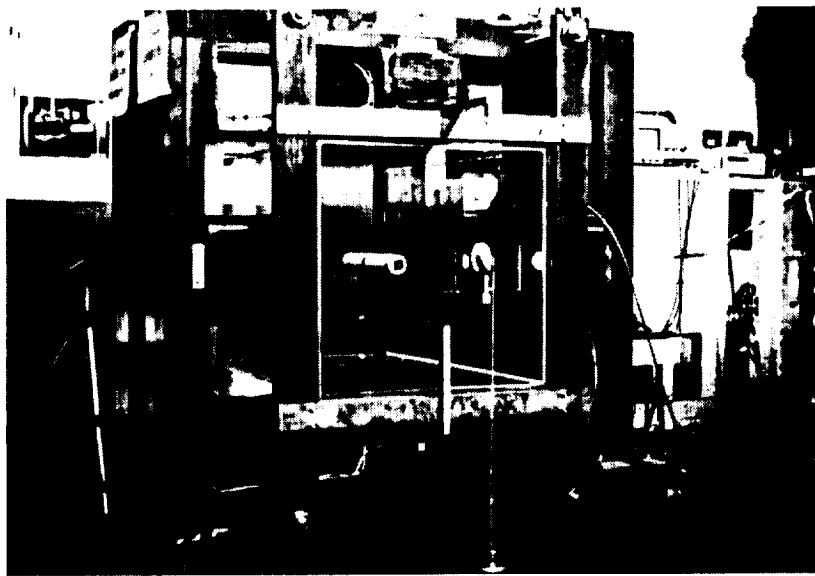


Figure 25 drag force calibration test

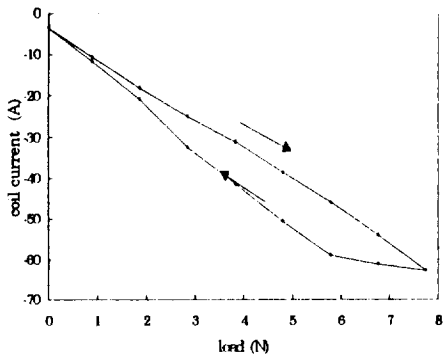


Figure 26 drag coil current vs. load (wide range)

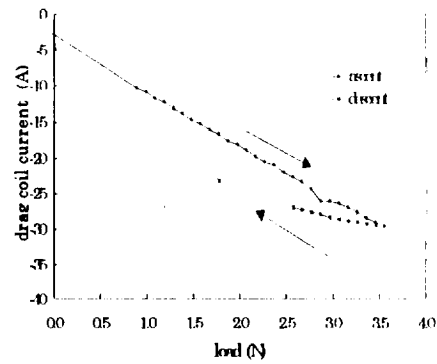


Figure 27 drag coil current vs. load (small steps)



**Session 14 -- Maglev 2**

Chairman: Tim Lynch  
Florida State University

